Toxicological assessment of mesoporous silica particles in the nematode *Caenorhabditis elegans*

Carolina Acosta,[a*] Jose M. Barat,[a] Ramón Martínez-Máñez,[b,c] Félix Sancenón,[b,c] Silvia Llopis,[d] Nuria González,[d] Salvador Genovés,[d] Daniel Ramón,[d] and Patricia Martorell[d]

[a]Grupo de Investigación e Innovación Alimentaria (CUINA) - Departamento de Tecnología de Alimentos. Universitat Politècnica de València, Valencia, Spain

[b]Instituto Interuniversitario de Investigación de Reconocimiento Molecular y Desarrollo Tecnológico (IDM). Universitat Politecnica de València and Universitat de València, Valencia, Spain

[c]CIBER de Bioingeniería, Biomateriales y Nanomedicina (CIBER-BBN), Spain

[d]Department of Food Biotechnology, Biopolis S.L., Parc Científic Universitat de València, Spain

*Corresponding author: cararo@upvnet.upv.es (CA)

¶ All Authors contributed equally to this work

‡ Conflict of interest: The authors declare that there is no competing financial interest and nothing to disclose.

Abstract

Here we report the toxicological evaluation of mesoporous silica particles (MSPs) in the nematode *C. elegans*. Specifically, we have investigated the effect of bare micro- (**M0**) and nano-sized (**N0**) MSPs, and their corresponding functionalized particles with a starch derivative (**Glu-N**) (**M1** and **N1**, respectively) on *C. elegans* ageing parameters. The toxicity of MSPs, their impact on *C. elegans* lifespan, movement capacity, progeny and ability to survive upon exposure to acute oxidative stress were assessed. This study demonstrated that both size particles assayed (**M0** and **N0**), labeled with rhodamine and monitored through fluorescence microscopy, are ingested by the nematode. Moreover, toxicity assays indicated that bare nano-sized particles (**N0**) have a negative impact on the *C. elegans* lifespan, reducing mobility and progeny production. By contrast, micro-sized particles (**M0**) proved innocuous for the nematodes. Furthermore, functionalization of nanoparticles with starch derivative reduced their toxicity in *C. elegans*. Thus, oral intake of **N1** comparatively increased the mean lifespan and activity rates as well as resistance to oxidative stress. The overall findings presented here demonstrate the influence of MSP size and surface on their potential toxicity *in vivo* and indicate the silica-based mesoporous particles to be a potential support for encapsulation in oral delivery applications. Furthermore, the good correlation obtained between healthy aging variables and viability (mean lifespan) validates the use of *C. elegans* as a multicellular organism for nanotoxicology studies of MSPs.

Keywords: Oral intake; Surface Functionalization; Mesoporous Silica; Nematodes; Lifespan; Healthspan.

1 Introduction

In recent years, inorganic nanomaterials have gained appeal as suitable supports for delivery applications [1]. Among inorganic supports for encapsulation and controlled release, mesoporous silica particles (MSPs) have received great interest [2–5]. MSPs have tunable and homogeneous pore size distribution (in the 2–10 nm diameter range), and high specific surface area and volume, which provide a large loading capacity [6-7]. Apart from being a porous structure, MSPs stand out for exhibiting a high concentration of structural defects on their surface in the form of silanol (Si-OH) groups, which can easily react with trialkoxysilane derivatives ((R'O)3-Si-R), enabling the generation of organic−inorganic hybrid supports [8-9]. This strategy offers a wide range of new perspectives in the design of on-command release particles to control the delivery of a previously entrapped guest [5, 10-12]. In accordance with this concept, the literature reports examples of MSPs functionalized with a number of different molecules and biomolecules able to deliver the cargo upon the application of various stimuli, such as physical (light, temperature, magnetic fields, ultrasounds) [13-17], chemical (anions, cations, neutral molecules, redox-active species and pH) [18-20] and biochemical (enzymes, DNA and antibodies) [21-24]. However, in spite of the promising applicability of MSPs, their toxic effect after oral administration is still poorly understood.

Among the biological models available, the nematode *Caenorhabditis elegans* has emerged as a well-suited *in vivo* system for toxicological studies due to its established biology and readily scorable life traits. *C. elegans* is a multicellular organism with a short lifespan (21 days). Experiments with *C. elegans* are less expensive than those carried out with vertebrate models and allow for a wide set of tests under different conditions in a short time span [25]. Moreover, results obtained with *C. elegans* can be predictive of those in higher eukaryotes because many physiological processes, signal transduction pathways and genes are conserved [26]. In addition, quantitative parameters of toxic effects on *C. elegans* can be easily determined through progeny production, mortality (lifespan), sensitivity to oxidative stress and changes in movement capacity (healthy aging evaluation). These features have led to an increase in the use of *C. elegans* as a suitable model in toxicological studies. Thus, recent toxicological studies with nanomaterials have been carried out in *C. elegans* [27-29]. Nonetheless, very few studies have been reported with *C. elegans* and silica-based particles. In particular, amorphous (non-porous) silica nanoparticles have been evaluated [30-31]. Our results suggest that non-porous silica nanoparticles (smaller than 50 nm) induce premature aging, causing progeny reduction and alterations in phenotypes related to aging. However, studies with *C. elegans* and MSPs are lacking, and there is an absence of correlation studies of lifespan and healthspan of nematodes fed with MSPs.

Taking into account the increasing interest in the design and use of mesoporous silica particles for delivery applications, we report herein the evaluation of toxicity of nano- and micro-sized MSPs based on *C. elegans* lifespan and healthspan analysis (movement capacity, resistance to acute oxidative stress and offspring production). Moreover, we studied the impact of functionalization of particles. The results show that surface functionalization of MSPs is a suitable procedure to significantly reduce the toxicity of nano-sized particles.

2 Materials and methods

2.1 Chemicals

All the chemicals were purchased at the highest possible grade available and were directly used with no further purification. Chemicals tetraethylorthosilicate (TEOS), cetyltrimethylammonium bromide (CTABr), sodium hydroxide, triethanolamine (TEAH), (3-aminopropyl)triethoxysilane (APTES) were provided by Aldrich. Hydrolyzed starch Glucidex® 47 (5% glucose, 50% maltose, 45% oligosaccharides and polysaccharides) was provided by Roquette.

2.2 *C. elegans* strain and maintenance

C. elegans strain Bristol (wild-type) N2 was obtained from the *Caenorhabditis* Genetics Center at the University of Minnesota and was maintained at 20°C on nematode growth medium (NGM). Also the *Escherichia coli* OP50 strain used as a normal diet for nematodes was obtained from the same culture collection.

2.3 Synthesis of micro-sized mesoporous silica particles (M0)

Micro-sized mesoporous silica particles were synthesized by the "atrane route" [32] in which 4.68 g of CTABr were added at 118 °C to a TEAH solution (25.79 g) that contained 0.045 mol of a silatrane derivative (TEOS, 11 mL). Next 80 mL of water were slowly added with vigorous stirring at 70 °C. After a few minutes, a white suspension was formed. This mixture was aged at room temperature overnight. The resulting powder (as- synthesized material) was collected by filtration and washed. The solid was dried at 70°C and was finally calcined at 550 °C for 5 h in an oxidant atmosphere in order to remove the template phase.

2.4 Synthesis of nano-sized mesoporous silica-based particles (N0)

Nano-sized mesoporous silica particles were synthesized by a well-known procedure [23]. Cetyltrimethylammoniumbromide (CTABr, 1.00 g, 2.74 mmol) was first dissolved in 480 mL of deionized water. Then 3.5 mL of a NaOH 2.00 mol L^{-1} solution were added, followed by an adjustment of temperature to 80 °C. TEOS (5.00 mL, 22.4 mmol) was then added dropwise to the surfactant solution. The mixture was stirred for 2 h to give a white precipitate. Finally, the solid was collected by centrifugation, washed with deionized water and dried at 70°C overnight (as-synthesized material). To prepare the final mesoporous nanoparticles (**N0**), the as-synthesized solid was calcined at 550 °C in an oxidant atmosphere for 5 h to remove the template phase.

2.5 Synthesis of the starch derivative (Glu-N)

According to Bernardos et al., a solution of APTES (5.85 mL, 25 mmol) was added to a suspension of hydrolyzed starch (Glucidex@ 47) in ethanol [23]. The reaction mixture was stirred for 24 h at room temperature and heated at 60°C for 30 min. The solvent was evaporated under reduced pressure [23].

2.6 Synthesis of starch-functionalized mesoporous silica particles (M1 and N1)

The starch-functionalized mesoporous silica particles **M1** and **N1**, was based on the protocol developed by Bernardos et al., [23]. **Glu-N** was added to **M0** and **N0** in a 1:1 w/w ratio at aqueous solution. The final mixture was stirred for 5.5 h at room temperature under argon. The solid was filtered, washed with abundant deionized water and dried for 12 h at 35 °C.

2.7 Synthesis of labeled particles (M0-rhd and N0-rhd)

Particles **M0** and **N0** were labeled with rhodamine B using a similar procedure to that reported by Xu and coworkers [33]. First the solid surface was modified with APTES. For this purpose, **M0** or **N0** nanoparticles were suspended in toluene (30 mL) and 0.19 mL of APTES (0.8 mmol) were added. The final suspension was refluxed at 110 °C for 20 h. Afterwards, 50 mg of the corresponding solid was suspended in ethanol with 50 mg B rhodamine isothiocyanate (RITC) for 20 h to obtain **M0-rhd** and **N0-rhd**.

Finally, ethanol suspensions were filtered and solids were washed with abundant deionized water, and dried for 12 h at 35 °C.

2.8 Material characterization

PXRD measurements were taken on a Seifert 3000TT diffractometer using CuKα radiation. TEM images were obtained under a 100 kV Philips CM10 microscope. Thermogravimetric analyses were carried out on a TGA/SDTA 851e Mettler Toledo balance in an oxidant atmosphere (air, 80 $mLmin^{-1}$) with a heating program that consisted of a heating ramp of 10 °C per minute from 120 to 1000 °C, and an isothermal heating step at this temperature for 30 min.

N_2 adsorption-desorption isotherms were recorded in a Micromeritics ASAP2010 automated sorption analyzer. Samples were degassed at 120 °C in vacuum overnight. The specific surface areas were calculated from the adsorption data within the low pressure range using the BET model [34].

Dynamic light scattering (DLS) studies for size distribution were conducted at 25 °C using a Malvern Zetasizer Nano ZS and Malvern Mastersizer 2000 (Malvern, U.K.). Data analysis was based on the Mie theory using refractive indices of 1.33 and 1.45 for the dispersant and MSP, respectively. To determine the zeta potential (ζ) of bare and functionalized MSP, a Zetasizer Nano ZS (Malvern Instruments, U.K.) was used. Zeta potential was calculated from the particle mobility values by applying the Smoluchowski model. The average of five recordings was reported as the zeta potential. All the measurements in Malvern Zetasizer Nano ZS and Malvern Mastersizer 2000 were performed at 20 °C in triplicate and samples were dispersed in M9 buffer at concentration of 1 $mg \cdot L^{-1}$. Before each measurement, samples were sonicated for 10 min to preclude potential aggregation.

2.9 Particle suspension

Particles **M0**, **M1**, **N0** and **N1** were UV-sterilized for 30 min. Then particles were dispersed at a known volume fraction of M9 buffer ($KHPO_4$ 3 g L^{-1}, Na_2HPO_4 6 g L^{-1}, NaCl 5 g L^{-1}, $MgSO_4$ 1 mmol), and disposed in an ultrasound bath with 2 pulses of 15 min to reduce particle aggregates. For better handling, dispersions were aliquoted and stored at -20 °C until used.

2.10 Lifespan assays in *C. elegans*

Synchronized young adult worms of the wild-type strain were cultured at 20 ºC for 21 days. For standard fed conditions (control population), worms were cultured in NGM plates seeded with *E. coli* OP50. Worms fed with MSPs were transferred to NGM plates supplemented with the corresponding particles solution (doses assayed: 0.5; 5.0; and 50 µg mL^{-1} of **M0**, **N0**, **M1** and **N1**). Ten nematodes per plate were moved periodically to fresh plates (ten plates per condition, 100 individuals per assay) and their viability was scored every 2 days. Nematodes were considered to be dead if they failed to respond to a platinum wire, and viability was evaluated as percentage of alive population. Three independent assays were carried out for each particle type.

2.11 Sensibility to oxidative stress of *C. elegans* fed with MSPs

To measure the survival rates of *C. elegans* after exposure to an acute oxidative stress, a method previously developed was used [35]. Synchronized young adult nematodes; which had hatched in NGM on the agar plates with *E. coli* OP50, and in the absence (control population) or presence of the corresponding particles (i.e. **M0**, **N0**, **M1** or **N1**) were used. After 5 days of growth at 20 °C, nematodes were transferred to MB medium plates (Basal medium: agar 17 g L^{-1}, sodium chloride 5.85 g L^{-1}, cholesterol 0.005 g L^{-1}) containing 2 mM H_2O_2, and were incubated for 5 h. In addition, a positive population was included, nematodes were seeded on NGM plates with the well-known antioxidant, ascorbic acid (vitamin C) at 10 µg mL^{-1} [35]. Then survival was measured. Each experiment was done with 70 individuals and evaluations were carried out in triplicate.

2.12 Healthspan parameters

Recent authors suggest that evaluating the quality of life of nematodes (healthspan) gives more information than lifespan extension alone. Parameters such as movement, pharyngeal pumping (feeding), and lipofuscin accumulation have been measured as healthspan parameters [36]. In this particular, two different physiological parameters over the life of the worms fed with MSPs were testing (movement capacity and offspring).

For all the studies, synchronized young adult (0-day adults) were selected and transferred to plates for each condition (three doses: 0.5, 5.0, 50 µg mL^{-1} of **M0**, **N0**, **M1** and **N1**). A control population (NGM) was also included.

Movement capacity was monitored as the total right bends achieved in 35 seconds. Synchronized nematodes (70 individuals) were incubated in each condition until the 2-day adult and 9-day adult and then transferred to NGM plates for movement determination. Mobility mean was defined as number of curves per worm. Evaluations were made in triplicate.

To quantify the offspring, synchronized nematodes were selected (25 per condition) and individually transferred to NGM plates daily for 5 days. The number of progeny (L1 larvae) laid in each plate was counted to determine the offspring. Experiments were performed in triplicate.

2.13 Fluorescence Microscopy

Suspensions of both **M0-rhd** and **N0-rhd** particles were prepared in M9 buffer, and added to the surface of NGM agar plates, already seeded with the *E. coli* OP50, to reach a concentration of 5 µg mL^{-1} of particles per plate. Synchronized nematodes (Ten nematodes per plate) were transferred to the plates (five plates per condition) and after 5 days of incubation, nematodes were placed in a sample-holder with 2 % agarose pads, and anesthetized with levamisol solution. One sample-holder per each plate was prepared (The total population, 50 nematodes were analyzed). Finally, DIC (Nomarsky) and epi-fluorescence digital images were acquired with an Eclipse 90i Nikon microscope (Nikon Corporation, Japan) with a 20x objective equipped with a digital camera (Nikon DS-5Mc) and a fluorescence filter TRITC (G-2E/C). Images (between 10 to 20 images per each sample-holder) were processed and analyzed by the Nis Elements BR 2.32 software (Nikon Corporation, Japan). Evaluation was done in triplicate.

2.14 Statistical analysis

Statistical analyses were carried out by means of one-way analysis of variance (ANOVA) using Statgraphics software. Survival curves were analyzed by Kaplan Meier model and compared using the log rank survival significance test with SPSS statistical software package.

3 Results and discussion

3.1 Synthesis and characterization of MSPs

Bare micro- (**M0**) and nano-sized (**N0**) MSPs were synthesized using reported procedures (*vide supra*). Moreover, both **M0** and **N0** particles were functionalized with hydrolyzed starch to obtain the corresponding micro- (**M1**) and nano-sized (**N1**) starch-functionalized particles. Functionalization was carried out by reaction of **M0** and **N0** with **Glu-N.** The derivative **Glu-N** was prepared by reaction of APTES (3-aminopropyl-triethoxysilane) with hydrolyzed starch (Glucidex@ 47) in ethanol (see Fig.1). The solids were thoroughly washed with water and dried before use. ^{1}H NMR spectrum of **Glu-N** was consistent with that described in the literature (See supplementary information Fig S1) [23]. Moreover, particles **M0** and **N0** were labeled with a red fluorescent dye (i.e. rhodamine B isothiocyanate, RITC) [33] to obtain **M0-rhd** and **N0-rhd**, respectively.

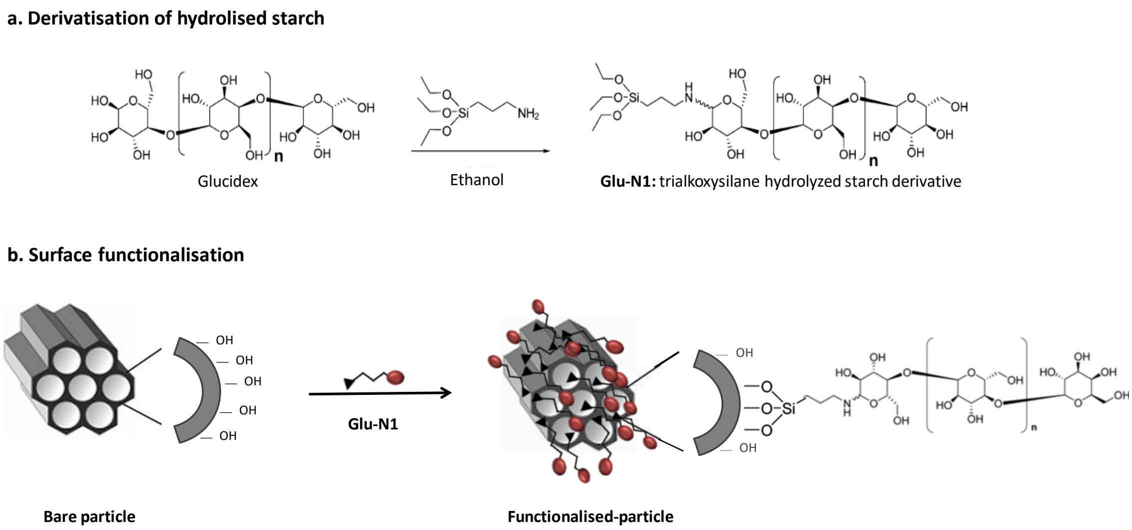

Figure 1. Synthesis of mesoporous silica particles capped with Glu-N.

The synthesized materials were characterized by standard techniques as described above. Powder X-ray diffraction (PXRD) patterns of bare **M0** and **N0** (as-synthesized and calcined) and starch-functionalized **M1** and **N1** particles are shown in Fig 2A. PXRD patterns of bare particles show the typical four low-angle reflections of mesoporous silica solids, which can be indexed as (100), (110), (200) and (210)

Bragg peaks. From the PXRD data, a_0 cell parameters of 47.89 and 49.73 Å (d100 spacing of 41.48 and 43.07 Å) were calculated for as-synthesized **M0** and **N0**, respectively. A significant shift of the (100) reflection in the PXRD in the calcined samples was clearly observed which corresponds to an approximate cell contraction of ca. 4.8 and 4.5 Å for calcined **M0** and **N0**, respectively (see Fig 2A). This is related to the condensation of silanols in the calcination step when CTABr was removed. For the starch-functionalized **M1** and **N1** particles, PXRD patterns showed only the characteristic (100) reflection. However, the presence of this peak clearly indicated that the mesoporous structure was preserved after anchoring of the **Glu-N** derivative. TEM images are also shown. For all particles, the typical porosity associated with this type of inorganic support is a pseudo hexagonal array of pore voids. Images provide evidence that **M0** and **M1** are irregular micrometric particles, whereas **N0** and **N1** are spherical nano-sized particles (see Fig 2B for typical TEM images of **M0** and **N0**).

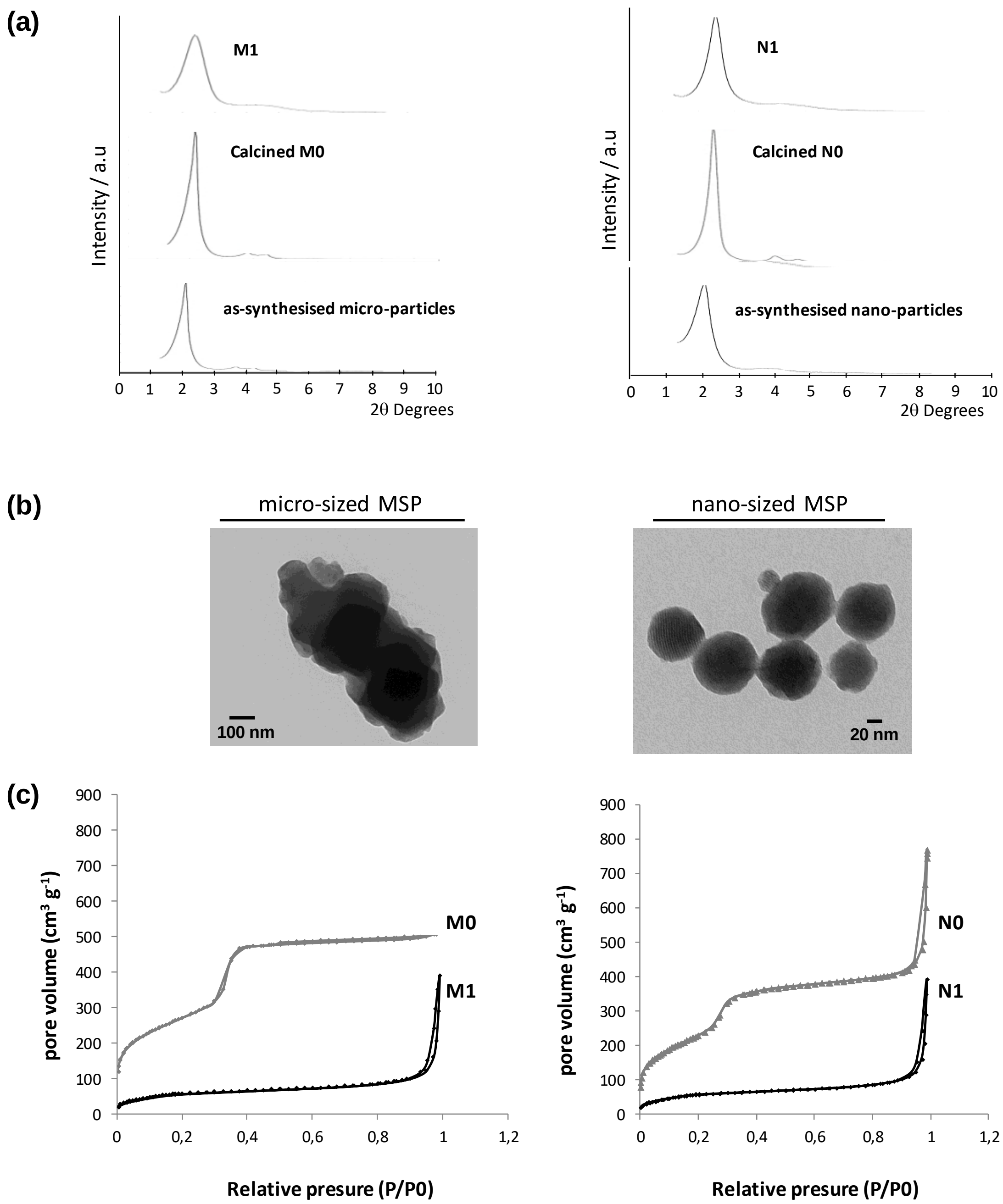

Figure 2. Materials characterization (a) Powder X-ray patterns (b) TEM images of micro-sized particles, M0 and nano-sized particles, N0 and (c) Nitrogen adsorption-desorption isotherms: Calcined material M0 [●], and Solid M1 [■]. Calcined material N0 [▲], and solid N1 [◆].

N_2 adsorption–desorption isotherms of **M0** and **N0** showed typical curves consisting of one single adsorption step at intermediate P/P0 values (0.1-0.4), which is related to nitrogen condensation inside mesopores by capillarity (Fig 2C). Absence of a hysteresis loop in this interval and a narrow pore distribution suggested the existence of uniform cylindrical mesopores with pore diameter and specific volume of, respectively, 3.19 nm and 0.78 cm^3 g^{-1} for **M0,** and 3.51 nm and 0.74 cm^3 g^{-1} for **N0** (calculated by the BJH model on the adsorption branch of the isotherm). The application of the BET model to calcined materials gave a total specific surface value of 979.6 m^2 g^{-1} and 843.9 m^2 g^{-1} for **M0** and **N0**, respectively. In contrast, N_2 adsorption–desorption isotherms of functionalized solids showed nearly flat curves when compared with un-functionalized starting materials. Due to the grafting of **Glu-N,** an appreciable reduction of porosity was observed. A specific surface area of 509.6 and 220.1 m^2 g^{-1} and pore volumes of 0.34 and 0.24 cm^3 g^{-1} were calculated for **M1** and **N1**, respectively. Table 1 lists BET specific surface values and pore volumes calculated from the N_2 adsorption-desorption isotherms.

Thermogravimetric analyses (TGA), zeta potential and size distribution studies were also performed. TGA curves of **M1** and **N1** showed a weight loss at 100-600°C due to the organic matter combustion that corresponded to the anchored starch derivative (see supplementary information Fig S2). From TGA analyses organic matter contents of 0.10 and 0.13 g per g SiO_2 for solids **M1** and **N1**, respectively, were calculated.

As particles were administered to worms in a buffered aqueous dispersion (M9 buffer for *C. elegans*, *vide infra*), zeta potential (ζ) and particle distribution sizes were determined in M9 buffer (Table 1). **M0** and **N0** treatment indicated a negative zeta potential due to the presence of anionic silanol groups on their surface. Upon functionalization, the surface potential changed from negative to positive, which was ascribed to the effective grafting of starch derivative **Glu-N** onto the surface of both materials. Dynamic light scattering (DLS) studies gave a mean size of 1930 nm for **M0** and of 1114 nm for **M1**, whereas mean sizes of 338 and 141 nm were found for **N0** and **N1**, respectively (see supplementary information Fig S3). When comparing size distribution and single-particle size, as determined by TEM (Table 1), mean particle size increased in the M9 buffer most likely as a result of partial particle aggregation, which agreed with previous studies [37].

Table 1. Characterization of the synthesized materials

	S_{BET} (m^2g^{-1})	pore volume (cm^3g^{-1})	Single-particle size (nm)*	Mean size (nm)§	Z potential (ζ) (mV)
M0	979.619^a	0.784^b	1566 ± 42^c	1930 ± 284 ^{d}	-18.60 ± 0.89 ^{e}
M1	509.591^a	0.343^b	1189 ± 81^c	1114 ± 133 ^{d}	11.06 ± 0.40 ^{e}
N0	843.899^f	0.741^g	97 ± 13	338 ± 11.82 ^{h}	-15.35 ± 2.14^i
N1	220.089^f	0.247^g	90 ± 13	141 ± 5.89 ^{h}	9.06 ± 0.28 ^{i}

*Single-particle size determined by TEM. § Mean size determined by Light Diffraction (dispersed in M9-buffer).
The same letters indicate significant differences between group memberships ($p < 0.05$).

Finally, as stated above, bare **M0** and **N0** were both labeled with rhodamine B isothiocyanate (RITC) using post-synthesis grafting procedure to obtain **M0-rhd** and **N0-rhd**, respectively [33]. A thermogravimetric evaluation indicated a rhodamine content of 4.8 % and 5.2 % in **M0-Rhd** and **N0-Rhd**, respectively.

3.2 Validation of oral intake of MSPs by *C. elegans*

Recent studies on *C. elegans* have confirmed the ability of nematodes to directly ingest inorganic nanomaterials [26-29]. In order to validate the ability of nematodes to ingest the different size of the synthetized MSPs, a monitoring study of the administered particles **M0-rhd** and **N0-rhd** was performed by means of fluorescent microscopy.

After particle suspension was seeded on plates, we hypothesized that particles would become available and could be swallowed by nematodes. After 5 days of **M0-rhd** and **N0-rhd** administration, nematodes were prepared for fluorescent microscopy and the oral intake of particles was monitored. Results showed that both **M0-rhd** and **N0-rhd** were ingested by nematodes and both particles were clearly located along the gastrointestinal tract (GIT) (Fig 3a and 3b). Both micro and nano-sized particles were located mainly in the lumen and pharynx. In addition, an uptake-gradient with a major concentration in the anterior intestine region was noticed, in agreement with results obtained in previous studies for other inorganic nanoparticles [30-31]. In order to evaluate the permanence of particles in the GIT and the ability of nematodes to excrete the ingested particles, 5-day old nematodes fed with **M0-rhd** and **N0-rhd** were divided into two groups. Group one (1) was prepared for fluorescence analyses as described above. To purge particles from nematodes, group two (2) was collected with M9-buffer and transferred to NGM plates without MSPs for 2 days. After this time, nematodes from group two (2) were prepared for fluorescent microscopy. Results strongly indicated the ability of *C. elegans* to ingest and excrete MSPs (Fig 3c and 3d). This was especially remarkable in nematodes fed with **N0-rhd** (Fig 2d), as nano-sized MSPs showed a higher trend to remain in the GIT, especially in the pharynx, when compared with micro-sized MSPs.

Although the resolution and sensitivity of the microscope limit the identification of endocytosis of particles, the lack of fluorescence outside the GIT of worms from group (2) suggested neither translocation nor accumulation of MSPs in secondary organs.

Finally, the progeny of nematodes fed with **M0-rhd** and **N0-rhd** was studied and no fluorescence was detected (see supplementary information Fig S4), suggesting that translocation of MSPs to the germ line did not occur.

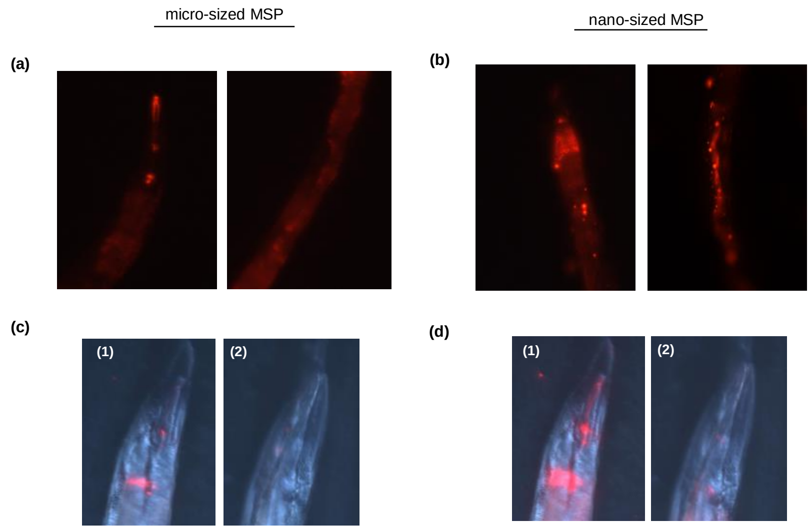

Figure 3. Particles monitored by fluorescence microscopy. (a) Nematodes fed with micro-sized MSPs, M0-rhd (b) Nematodes fed with nano-sized MSPs N0-rhd. To evaluate permanence of particles, worms were divided in group (1) and group (2). Group (1) remain with particles and group (2) were collected with M9-buffer for purging particles (c) Comparison from group (1) to group (2) of nematodes fed with micro-sized, M0-rhd and (d) Comparison from group (1) to group (2) of nematodes fed with nano-sized, N0-rhd.

3.3 Influence of MSPs size on their toxicity to *C. elegans*

The effect of **M0** and **N0** MSPs on *C. elegans* lifespan was analyzed. By using the above mentioned procedure to seed MSPs on agar plates, nematodes were fed throughout their life expectancy with three doses (0.5, 5 and 50 μg ml^{-1}) of **M0** and **N0**. In parallel, nematodes fed only on bacterial feed were evaluated as the control population. Survival curves and mean lifespan (defined as the time when 50 % of worms were dead) were obtained.

Results showed that both control population and nematodes fed with **M0** displayed a similar lifespan at the three doses assayed, obtaining very similar survival curves (see Supplementary information Fig S5). Thus, mean lifespan of **M0**-fed nematodes was similar to control-fed nematodes (Fig 4a). Only a slight but non-significant reduction was observed in mean lifespan with the higher dose (50 μg·mL^{-1}), probably due to a reduction in the comfort of nematodes due to the high density of microparticles in the agar.

In contrast, mean lifespan was significantly reduced at the three **N0** doses compared to the control population (p-values: 0.001; 0.007 and 0.002, for 0.5; 5.0; and 50 μg·ml^{-1}, respectively) (Fig 4a). Moreover, survival curves showed a shortened lifespan for worms fed with **N0** at the three doses assayed (see supplementary information Fig 6S). These results clearly indicate that smaller particles are harmful for *C. elegans,* because a significant reduction in nematode survival was observed (Fig 4b).

In order to further analyze the impact of feeding nano and micro-sized MSPs by nematodes, the movement capacity of *C. elegans* exposed to MSPs was evaluated. Previous research draws a connection between declining body movement and premature aging [30-31].

Therefore, movement capacity (quantified as the total right bends per minute) of 2-day adult worms (Fig 4c) and 9-day adults (Fig 4d) was evaluated in *C. elegans* fed with 0.5, 5 and 50 μg ml^{-1} of **M0** and **N0** respectively, and compared with the control population.

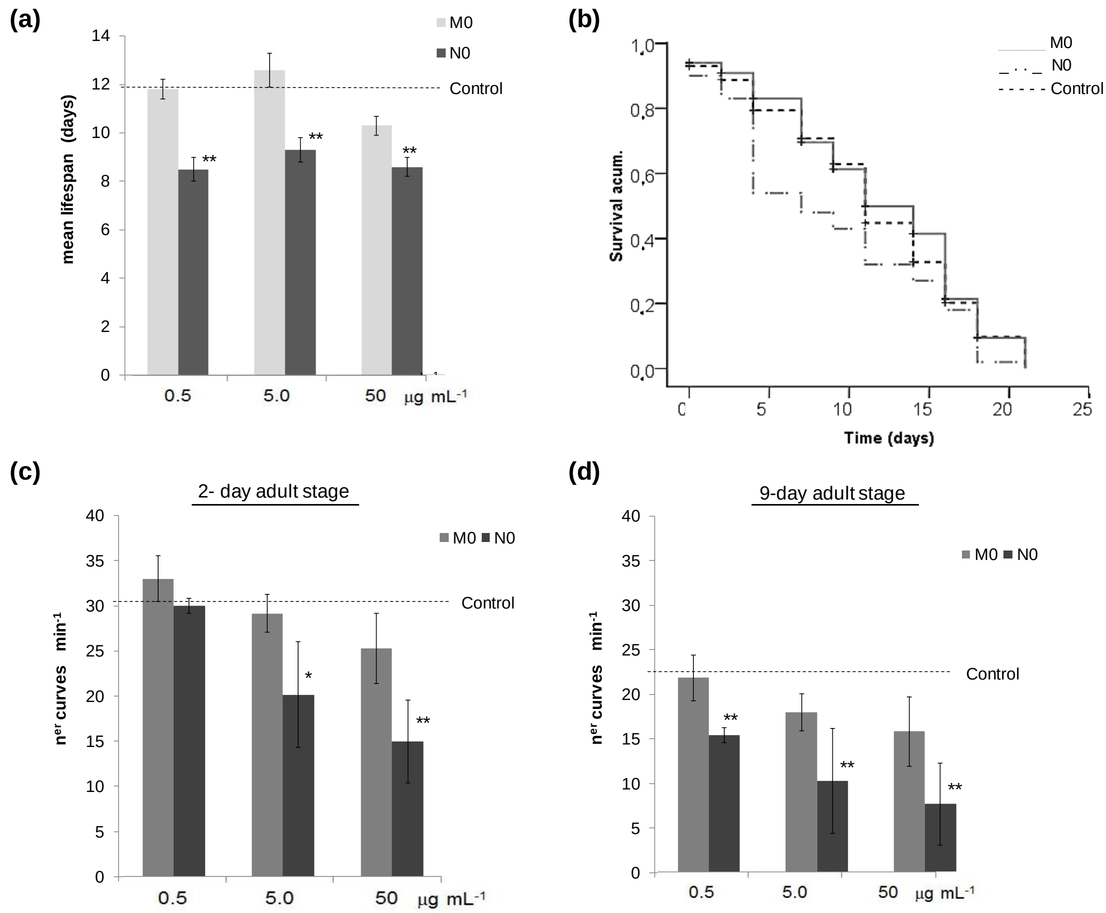

Figure 4. Evaluation of *C. elegans* orally administered with bare micro- (M0) and nano- (N0) sized MSPs. (a) Mean lifespan of three MSPs doses, (X axis 0.5; 5 and 50 µg·mL^{-1}). (b) Survival curves of nematodes fed with dose of 0.5 µg·mL^{-1}. (c) Movement capacity at 2-day adult stage and (d) at 9-day adult stage. (Significant differences for * p< 0.05 and **p<0.01)

In 2-day adult, the movement capacity of nematodes fed with low **M0** doses did not differ from that of the control population (Fig 4c). Slightly reduced movement rates were noticed in worms fed with 50 μg ml^{-1} of **M0,** but this was not statistically significant. In contrast, the effect of **N0** on depletion of movement was already evident and was significant in a dose-response manner (p-value: 0.08 and 0.01 for the 5 and 50 μg·ml^{-1}, respectively) (Fig. 4c).

On the assumption that as worms age, their motility begins to progressively slow down, the movement of 9-day adults was quantified. The movement capacity of nematodes fed with **M0** showed a similar number of curves per minute compared to the control population (Fig 4d). However, a significant reduction in movement capacity was also clearly evident in nematodes fed with **N0** (p-values for 9-day adults: 0.05, 0.01 and 0.002 for 0.5; 5.0; and 50 $\mu g \cdot ml^{-1}$, respectively).

The changes noted in movement capacity of **N0**-fed nematodes suggested that bare mesoporous silica nano-sized particles have a toxic-impact on *C. elegans*, which is also in agreement with the observed reduction in lifespan. Taking into account that movement depletion can be associated with neuronal damage [38, 39], our results could indicate a negative effect of nanoparticles on cognitive status. This clearly contrasts with micro-sized MSPs, which have no significant effect on nematodes' movement or lifespan.

3.4 Effect of surface functionalization on MSPs toxicity

The hypothesis of improving biocompatibility of inorganic nanomaterials through surface functionalization has been previously evaluated [40-43]. Evidence from studies in human cell cultures has revealed that surface modification by anchoring organic groups in silica-based particles may modulate toxicity and may mitigate undesirable biological effects [44]. Thus, we evaluated **M1** and **N1**-fed *C. elegans* in terms of lifespan and movement capacity.

There was no appreciable reduction in the lifespan of **M1**-fed worms compared with the control population (without particles); nor were there significant differences between **M0** and **M1** (Fig 5A). However, remarkable differences were found between nematodes fed with **N0** and **N1** (p-value: 0.017), (see Fig 5B). As stated above, mean lifespan of **N0**-fed nematodes was significantly reduced compared to the control population, whereas mean lifespan of **N1**-fed *C. elegans* was comparatively higher than **N0** (see supplementary information Table S1) being similar to that of the control population. This indicates a remarkable positive effect of coating nano-sized MSPs with the starch derivative.

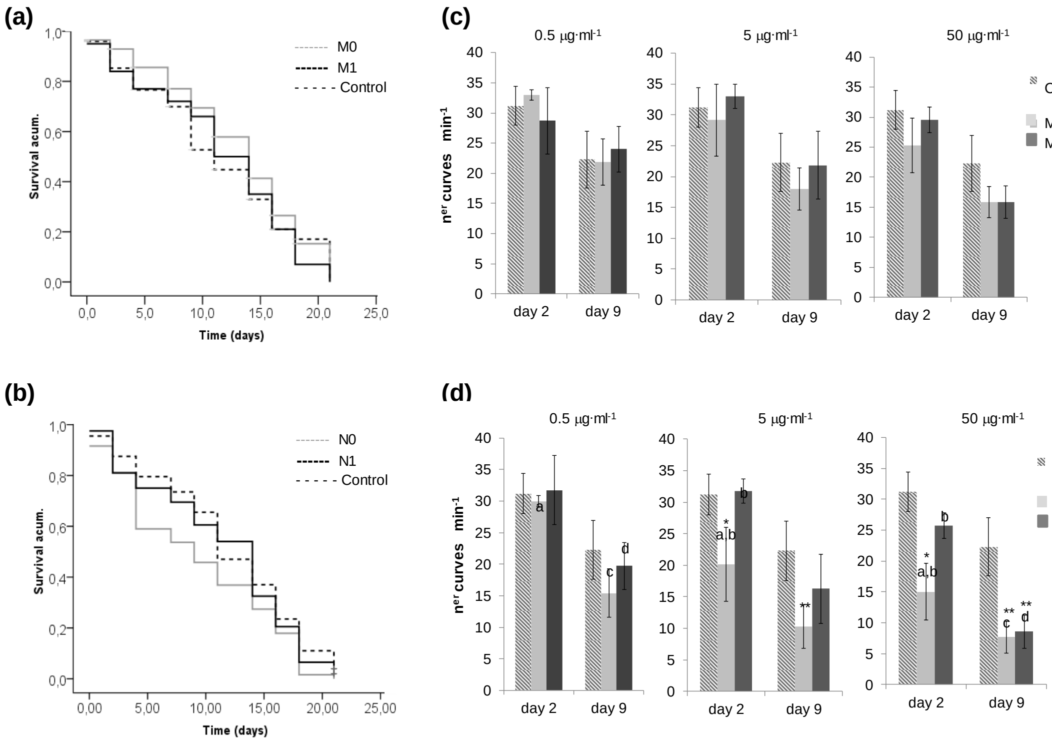

Figure 5. Influence of MSP surface functionalization on *C. elegans* toxicity. (a) Lifespan assays were carried out with 5 µg mL^{-1} of particles M0 and M1, and (b) N0 and N1 (Lifespan with other concentrations, in Supporting information, Figures S7 and S8). Movement capacity analysed as the mean speed (n^{er} curves/min) of worms fed with different concentrations of (c) M0 and M1 and (d) N0 and N1. Significant differences p < 0.01.

Regarding movement capacity of *C. elegans*, no significant differences were found between nematodes fed with **M0** and **M1** (Fig 5c), whereas a significant increase in mobility was determined in **N1**-fed nematodes compared with **N0**-fed worms (see Fig 5d). This observation was specifically significant in 2-day-old adult nematodes fed with 0.5; 5 and 50 µg ml^{-1} of **N1** (p-value: 0.002) and also in 9-day-old adult nematodes fed with 0.5 and 5 µg ml^{-1} (p-value: 0.015). In contrast, the 9-day-old adult nematodes fed with 50 µg ml^{-1} **N0** or **N1** displayed a similar movement capacity, which suggests that the positive starch functionalization effect observed in young adult nematodes became less effective as they aged, especially when using a large concentration of the nanoparticles.

The above lifespan and movement capacity data are well correlated. Results demonstrate that toxicity of mesoporous silica particles is related to particle size and doses, and may be reduced by surface functionalization. Regarding nematode body movement, some authors have pointed out that depletion in movement is associated with a reduction in motor function, muscle structure and cellular deterioration [38-39]. Therefore, it could be hypothesized that functionalization with starch modifies the way nano-sized particles interact and influence functions in nematodes resulting in less toxicity. When compared to bare nanoparticles, the functionalization of the mesoporous silica nanoparticles with (**Glu-N**) improved biocompatibility and induced a recovery in lifespan and movement capacity of *C. elegans*.

Taking into account that nano-sized particles can produce toxicity in *C. elegans*, we further studied other health-related variables, such resistance to oxidative stress and offspring. In *C. elegans*, a positive connection between lifespan and stress-resistance has been demonstrated for a variety of studies [45-46]. Nematode survival rate after H_2O_2-induced oxidative stress was determined in a population fed with bare and functionalized nano- (**N0** and **N1**) particles. The control population was seeded on NGM plates with only bacterial food, and as state above (section 2.11), the positive population was placed on NGM plates with antioxidant ascorbic acid (10 µg mL^{-1}) added along with bacterial food. In accordance with previous results, *C. elegans* fed with **N1** showed better resistance to oxidative stress than those fed with **N0** (p-value: 0.009 and 0.029 to 0.5 and 5 µg·ml^{-1}, respectively), see Fig 6a.

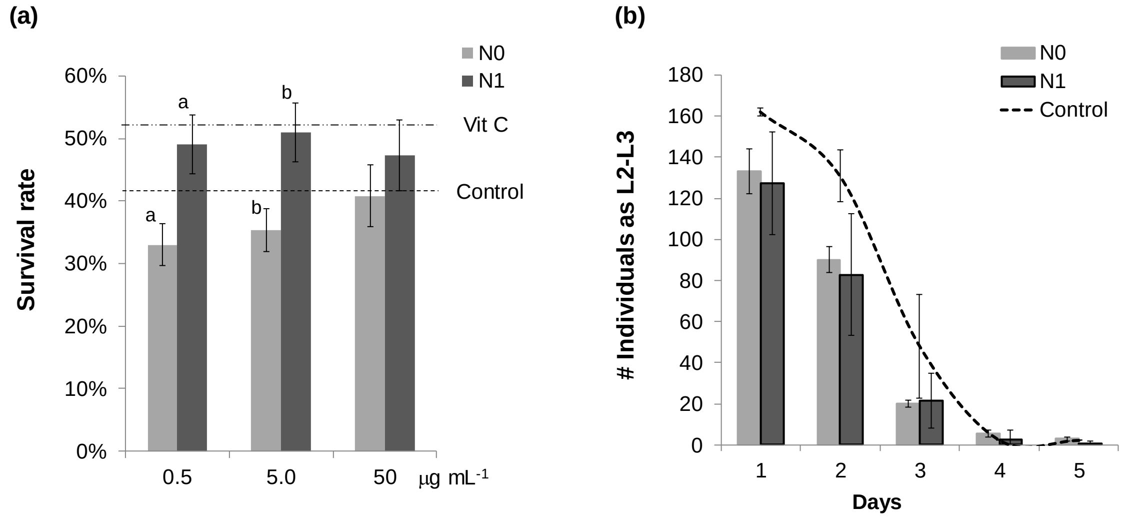

Figure 6. a) Resistance to oxidative stress in the worms fed with nano-size MSPs (Bare and functionalized N0 and N1, respectively). Three doses were evaluated (X axis) 0.5; 5 and 50 µg·ml^{-1}. b) Progeny distribution decreased on day 2 in worms fed at 5 µg.ml^{-1} with bare nano-sized (N0) and functionalised (N1) MSPs.

We hypothesized two mechanisms by which MSPs may affect nematodes' sensitivity to acute oxidative stress. On the one hand, the presence of small particles could influence the nematode's ability to respond to acute stress due to the fact that nano-sized particles may affect the metabolism related with reactive oxygen species (ROS) formation. Moreover, bare particles have more exposed silanols groups, which could affect nematode functions. On the other hand, membrane receptors could change their response (activate or suppress signal cascades) according to the stress factors present in the agar plate, which does not always behave as a linear response. This could explain why higher doses of smaller particles (**N0**) did not affect stress resistance. Hence, it is worth highlighting the positive effect on the nematodes fed with **N1**, which reached the response of nematodes fed with the antioxidant compound (Vitamin C).

Apart from a reduction in resistance to oxidative stress, previous studies on *C. elegans* have shown that particles smaller than 50 nm, directly affect ovoposition. This is due to the translocation of the nanoparticles from primary organs, such as epithelial cells of the intestine, to secondary organs that belong to the reproductive tract. Findings showed that mainly amorphous (non-porous) silica particles accumulate and block certain organs, such as the vulva, inducing egg hatching inside the parent's body [30]. By contrast, the present study evaluated mesoporous-silica and relatively larger particles (nano-sized MSPs are in a size range of 80-100 nm), and MSP accumulation was not observed in the vulva or in the germ line (*vide ante*); however, an additional progeny analysis was performed on worms fed with bare and functionalized nano-sized MSPs.

Laid eggs and the subsequent progeny of nematodes fed with three different doses of **N0** and **N1** particles were measured. Progeny distribution of nematodes fed with doses of 5 $\mu g \cdot ml^{-1}$ is shown in Fig 6b (to see the effect of additional dose see supplementary information Fig. S9).

Progeny evaluation indicated that control population adults laid the most progeny on day 1 and that the offspring rate decreased on days 2 and 3 (Fig 6b). Results suggest that nanoparticles generate acute stress on fertility because ovoposition was significantly affected from day 1 to adult day 2. In particular, nematodes fed with **N0** showed a significantly lower oviposition rate on adult day 2 compared to the control population (p-value: 0.01). In contrast, nematodes fed with **N1** showed a minor depletion, which was not significant compared with the control population (p-value: 0.6). This indicates that functionalized particles slightly improve the reproductive status of nematodes.

Since there was no reason to associate progeny depletion with accumulation of MSPs in the vulva, we suggested that the functions associated with fertility could be more sensitive to external stress due to exposure to nano-sized MSPs. It could somehow be related to the depletion of healthspan variables, which agrees with previous reports, where nervous parameters were related with movement and egg-laying phenotypes [31]. In any case, the healthspan evaluation performed in *C. elegans* provides an interesting methodology for evaluating the influence of the MSP surface modification on nanotoxicity. Nonetheless, more extensive studies into phenotype expressions and stress biomarkers would be of interest and will be carried out.

4 Conclusions

Here we show the feasibility of using *C. elegans* as *in vivo* model to evaluate the toxicity of MSPs. The intake of micro and nano-sized MSPs has been demonstrated, with accumulation occurring mainly in the gastrointestinal tract and the pharynx. Evaluation of lifespan and other age-related parameters in nematodes exposed to micro and nanoparticles has demonstrated the safety of micro-sized MSPs. By contrast, the toxicity of nano-sized MSPs has been shown through the decrease in lifespan, reduction of movement, depletion of reproductive status and an increase in sensitivity to oxidative stress. Furthermore, our study shows that starch-functionalized mesoporous silica nanoparticles (**N1**) have no significant effect on the lifespan and healthspan of *C. elegans*. These results strongly suggest that surface functionalization of MSPs is a suitable strategy to reduce toxicity and enhance biocompatibility of the smallest particles.

Acknowledgments

The authors wish to express their gratitude to the Spanish Government (MINECO Projects AGL2012-39597-C02-01, AGL2012-39597-C02-02, AGL2015-70235-C2-1, MAT2012-38429-C04-01 and MAT2015-64139-C4-1), the Generalitat Valenciana (Project PROMETEOII/2014/047) and Colombian Administrative Department of Science, Technology and Research which supported Ms. Acosta Scholarship. We would also like to thank the Institut de Ciència dels Materials (ICMUV), the Microscopy Service of the Universitat Politècnica de València and the microscopy service of IATA for technical support. We thank Roquette for the Glucidex samples.

References

[1] Mo R, Jiang T, Di J, Tai W and Gu Z. Emerging Micro- and nanotechnology based synthetic apporaches for insulin delivery. Chem. Soc. Rev. 2014;43:3595–629.

[2] Valtchev V, Tosheva L. Porous Nanosized Particles: Preparation, Properties, and Applications. Chem. Rev, 2013;113:6734-6760.

[3] Stein A. Advances in Microporouss and Mesoporous Solids- Highlights of Recent Progess.Adv. Mater, 2003;15:763-775.

[4] Soler-Illia G-JAA, Azzaroni O.Multifunctional hybrids by combining ordered mesoporous materials and macromolecular building blocks. Chem. Soc. Rev 2011;40:1107-1150.

[5] Angelos S, Johansson E, Stoddart JF, Zink JI. Mesostructured Silica Supports for Functional Materials and Molecular Machines. Adv. Func. Mater2007;17:2261-2271.

[6] Salonen J, Lehto V-P. Fabrication and chemical surface modification of mesoporous silicon for biomedical applications. Chem. Eng. J 2008;137:162–172.

[7] Wight AP, Davis ME. Design and Preparation of Organic-Inorganic Hybrid Catalysts. Chem. Rev2002;102:3589-3614.

[8] Vinu A, Hossain KZ, Ariga K. Recent Advances in Functionalization of Mesoporous Silica. J. Nanosci. Nanotechnol. 2005;5:347–371.

[9] Kickelbick G. Hybrid inorganic-organic mesoporous materials. Angew. Chem. Int. Ed. 2004;43:3102-3104.

[10] Coll C, Bernardos A, Martínez-Máñez R, Sancenón F. Gated silica mesoporous supports for controlled release and signaling applications. Acc. Chem. Res. 2013;46:339-349.

[11] Aznar E, Oroval M, Pascual Ll, Murguía JR, Martínez-Máñez R, Sancenón F. Gated Materials for On-Command Release of Guest Molecules. Chem. Rev 2016;116:561-718.

[12] Sancenón F, Pascual Ll, Oroval M, Aznar E, Martínez-Máñez R. Gated Silica Mesoporous Materials in Sensing Applications. ChemOpen 2015;4:418-437.

[13] Mal NK, Fujiwara M, Tanaka Y, Taguchi T, Matsukata M. Photoswitched storage and release of guest molecules in the pore void of coumarin-modified MCM-41. Chem. Mater. 2003;15:3385-3394.

[14] Agostini A, Sancenón F, Martínez-Máñez R, Marcos MD, Soto J, Amorós P. A photoactivated molecular gate. Chem. Eur. J. 2012;18:12218–12221.

[15] Fu Q, Rao VR, Ista LK, Wu Y, Andrzejewski BP, Sklar LA, Ward TL, López GP. Control of molecular transport through stimuli-responsive ordered mesoporous materials. Adv. Mater. 2003;15:1262–1266.

[16] Aznar E, Mondragón L, Ros-lis JV, Sancenón F, Marcos MD, Martínez-Máñez R, Soto J,Pérez-Payá E, Amorós P. Finely tuned temperature-controlled cargo release using paraffin-capped mesoporous silica nanoparticles. Angew. Chem. Int. Ed. 2011;50:11172–11175.

[17] Giri S, Trewyn BG, Stellmaker MP, Lin VSY. Stimuli-Responsive Controlled-Release Delivery System Based on Mesoporous Silica Nanorods Capped with Magnetic Nanoparticles. Angew. Chem. Int. Ed. 2005; 44:5038–5044.

[18] Fujiwara M, Terashima S, Endo Y, Shiokawa K, Ohue H. Switching catalytic reaction conducted in pore void of mesoporous material by redox gate control.Chem. Commun. 2006;44:4635–4637.

[19] Angelos S, Khashab NM, Yang YW, Trabolsi A, Khatib HA, Stoddart JF, Zink JI. pH clock-operated mechanized nanoparticles.J. Am. Chem. Soc. 2009;131:12912–12914.

[20] Casasús R, Climent E, Marcos MD, Martínez-Máñez R, Sancenón F, Soto J, Amorós P, Cano J. Dual aperture control on pH- and anion-driven supramolecular nanoscopic gate-like ensambles. J. Am. Chem. Soc. 2008;130:1903–1917.

[21] Oroval M, Climent E, Coll C, Erijta R, Aviñó A, Marcos MD,Sancenón F, Martínez-Máñez R, Amorós P. An aptamer-gated silica mesoporous material for thrombin detection.*Chem. Commun.* 2013;**49**:5480–5482.

[22] Schlossbauer A, Kecht J, Bein T. Biotin-Avidin as a protease-responsive cap system for controlled guest release from colloidal mesoporous silica.*Angew. Chem. Int. Ed.* 2009;**48:**3092–3095.

[23] Bernardos A, Mondragon L, Aznar E, Marcos MD, Martínez-Máñez R, Sancenón F, Soto J, Barat JM, Perez-Paya E, Guillem C, Amoros P. Enzyme-responsive intracellular controlled release using nanometric silica mesoporous supports capped with "saccharides".*ACS Nano*,2010;**4:**6353–6368.

[24] Park C, Kim H, Kim S, Kim C. Enzyme responsive nanocontainers with cyclodextrin gatekeepers and synergistic effects in release of guests.*J. Am. Chem. Soc.* 2009;**131**:16614–16615.

[25] *C. elegans* S. Consortium. Genome sequence of the nematode *C. elegans*: a platform for investigating biology, *Science.* 1998;**282:**2012–8.

[26] Leung MCK, Williams PL, Benedetto A, Au C, Helmcke KJ, Aschner M, Meyer JN. *Caenorhabditis elegans*: An emerging model in biomedical and environmental toxicology.*Toxicol. Sci.* 2008;**106**:5–28.

[27] Cha Y.J, Lee J, Choi S.S. Apoptosis-Mediated In Vivo Toxicity of Hydroxylated Fullerene Nanoparticles in Soil Nematode *Caenorhabditis Elegans*. *Chemosphere* 2012;**87**:49–54.

[28] Wang H, Wick R.L, Xing B. Toxicity of Nanoparticulate and Bulk ZnO, Al_2O_3 and TiO_2 to the Nematode *Caenorhabditis Elegans*. *Environ. Pollut*. 2009;**157**:1171–1177.

[29] Gonzalez-Moragas L, Roig A, Laromaine A.*C. Elegans* as a Tool for In Vivo Nanoparticle Assessment. *Adv. Colloid Interface Sci*. 2015;**219**:10–26.

[30] Pluskota A, Horzowski E, Bossinger O, von Mikecz A. In *Caenorhabditis elegans* nanoparticle-bio-interactions become transparent: silica-nanoparticles induce reproductive senescence.*PLoS One* 2009;**4**: e6622.

[31] Scharf A, Piechulek A, von Mikecz A.Effect of nanoparticles on the biochemical and behavioral aging phenotype of the nematode *Caenorhabditis elegans*.*ACS Nano* 2013;**7**:10695–10703.

[32] Cabrera S, El Haskouri J, Guillem C, Latorre J, Beltrán A, Beltrán D, Marcos MD,Amorós.Generalised syntheses of ordered mesoporous oxides: the atrane route.*Solid State Sci.* 2000;**2:**405–420.

[33] Xu C, Niu Y, Popat A, Jambhrunkar S, Karmakar S, Yu C. Rod-like mesoporous silica nanoparticles with rough surfaces for enhanced cellular delivery.*J. Mater. Chem. B* 2014;**2**:253–256.

[34] Brunauer S, Emmett PH, Teller E. Adsorption of gases in multimolecular layers. *J. Am. Chem. Soc.* 1938;**60**:309–319.

[35] Martorell P, Bataller E, Llopis S, Gonzalez N, Álvarez B, Montón F, Ortiz P, Ramón D, Genovés S. A cocoa peptide protects Caenorhabditis elegans from oxidative stress and beta-amyloid peptide toxicity. *Plos One.* 2013;**8 (5)**:e63283

[36] Bansal A, Zhu L, Yen K, Tissenbaum H.. Uncoupling lifespan and healthspan in Caenorhabditis elegans longevity mutants. *PNAS.* 2015:E277-E286[37] Pérez-Esteve E, Oliver L, García L, Nieuwland M, De Jongh HHJ, Martínez-Máñez R, Barat JM.*Langmuir* 2014;**30**:6970–6979.

[38] Garigan D, Hsu A-L, Fraser AG, Kamath RS, Ahringer J, Kenyon C. Genetic analysis of tissue aging in *Caenorhabditis elegans*: a role for heat-shock factor and bacterial proliferation.*Genetics* 2002;**161**:1101-1112.

[39] Herndon L, Schmeissner P, Dudaronek J, Brown P, Listner K, Sakano Y, Paupard MC, Hall D, Driscoll M. Stochastic and genetic factors influence tissue-specific decline in ageing *C. elegans*.*Nature* 2002;**419**:808–14.

[40] Wu EC, Andrew JS, Buyanin A, Kinsella JM, Sailor MJ. Suitability of porous silicon microparticles for the long-term delivery of redox-active therapeutics.*Chem. Commun.*2011;**47**:5699–5701.

[41] Caballero-Díaz E, Pfeiffer C, Kastl L, Rivera-Gil P, Simonet B, Valcárcel M, Jiménez-Lamana J, Laborda F, Parak WJ. The Toxicity of Silver Nanoparticles Depends on Their Uptake by Cells and Thus on Their Surface Chemistry.*Part. Part. Syst. Charact.* 2013;**30**:1079–1085.

[42] Santos HA, Riikonen J, Salonen J, Mäkilä E, Heikkilä T, Laaksonen T, Peltonen L, Lehto VP, Hirvonen J. *In vitro* cytotoxicity of porous silicon microparticles: effect of the particle concentration, surface chemistry and size.Acta Biomater. 2010;6:2721-31.

[43] Bimbo LM, Sarparanta M, Santos HA, Airaksinen AJ, Mäkilä E, Laaksonen T, Peltonen L, Lehto VP, Hirvonen J, Salonen J.Drug permeation across intestinal epithelial cells using porous silicon nanoparticles.*ACS Nano* 2010;**4**:3023–3032.

[44] Lankoff A, Arabski M, Wegierek-Ciuk A, Kruszewski M, Lisowska H, Banasik-Nowak A, Rozga-Wijas K, Wojewodzka M, Slomkowski S.Effect of surface modification of silica nanoparticles on toxicity and cellular uptake by human peripheral blood lymphocytes *in vitro*.*Nanotoxicology* 2013;**7**:235–50.

[45] Amrit F, May R.Younger for longer: insulin signalling, immunity and ageing.*Curr. Aging Sci.* 2010;**3**:166–76.

[46] Grompone G, Martorell P, Llopis S, González N, Genovés S, Mulet AP, Fernández-Calero T, Tiscornia I, Bollati-Fogolín M, Chambaud I, Foligné B, Montserrat A, Ramón D. Anti-inflammatory Lactobacillus rhamnosus CNCM I-3690 strain protects against oxidative stress and increases lifespan in *Caenorhabditis elegans*.*PLoS One* 2012;**7**:e52493.

Supporting information

S1 Fig.Glu-N^{1}H-NMR spectrum.

S2 Fig. TGA for solids M1 and N1.

S3 Fig. S**ize distribution of particles.**

S4 Fig. Progeny image of worms fed with M0-rhd and N0-Rhd. S

S5-S8 Fig Address lifespan curves of worms fed with M0 (S5 Fig), N0 (S6 Fig), M0-M1 (S7 Fig) and N0-N1 (S8 Fig).

S9 Fig. **Progeny distribution of worms fed with MSP.**

S1 Table. Mean lifespan results